

# Edge preserved denoising and singularity extraction from angles gathers

Felix Herrmann, ERL, MIT and Maarten de Hoop, CWP, CSM

## Summary

A matching pursuit technique composed with an imaging method is used to obtain quantitative information on geological records from seismic data. The technique is based on a greedy non-linear search algorithm decomposing data into atoms. These atoms are drawn from a redundant dictionary of seismic waveforms. Fractional splines are used to define this dictionary, whose elements are not only designed to match the observed waveforms but also to span the appropriate family of geological patterns. Consequently, the atom's parameterization provides localized scale, order and direction information that reveals the stratigraphy and the type of geological transitions. Besides a localized scaling characterization, the atomic decomposition allows for an accurate denoised reconstruction of data with only a small number of atoms. Application of this approach to angles gathers allows us to track geological singularities from seismic data. Our characterization bridges the gap between the analysis of the main features within geologic processes, i.e. the geologic patterns, and the interpretation of their associated seismic response. A case study of Valhall data is presented.

## Introduction

The history of geological processes is stored in geological records. On their turn, changes in the geological record are manifest in the elastic moduli and their spatial distribution. Abrupt changes in the elastic moduli, also known as singularities, correspond to important features within geological processes and occur mostly in the vertical direction. Seismic measurements provide access to these features because seismic waves predominantly interact at these singularities in the elastic moduli and/or density.

In this paper we present a method of recovering the geologic record from seismic data. First, we transform seismic data into a collection of images parametrized by angles. Under certain conditions, the angles within these scattering angles common image gathers (CIG's) correspond to the angles under which the sub-surface singularities are being insonified by the seismic waves (Brandsberg-Dahl and de Hoop, 1998). Second, we subject these images to an adaptive atomic decomposition in one spatial direction, generally the vertical, and then perform this procedure for each of the remaining spatial directions, generally the horizontal. Inherent redundancy of the angles domain data is utilized by submitting the angles CIG's to a non-adaptive wavelet thresholding (Donoho and Johnstone, 1998) along the angles coordinates. This thresholding denoises the images and enforces smoothness in the angle directions. Conversely, we preserve the singularities in the depth-direction by a decomposition into transition sharpness-adaptive atoms. Noise in the data is removed because the decomposition extracts only the coherent structures. The parameterization of the selected atoms provides precise information on the location and shape of the important patterns within the geologic record.

As shown by Muller et al. (1992) and later by Herrmann (1997) sedimentary records show evidence of multifractal behavior, which means that these records consist of a wide variety of transitions with differing scaling/singular behavior (Herrmann, 2001b; Herrmann et al., 2001). The scale/Hölder exponents characterize the transition sharpness and vary discontinuously with position. Finding these exponents from bandwidth limited data is difficult because the lack of scales and the presence of noise. Therefore, we propose a method capable of estimating singularity orders from noisy data with limited scale content. The method is based on the identification of geological patterns by searching a redundant dictionary for waveforms that optimally correlate with seismic reflection events. The success of this atomic decomposition (Mallat, 1997) depends on how well the constructed elements, within the dictionary, match with generic geological transitions and their induced reflectivity.

Multifractal scaling of sedimentary records motivates a data-adaptive atomic representation by fractional spline wavelets, indexed by location, dyadic scale, direction, and a continuously varying scaling/regularity parameter. The scaling parameter measures the abruptness of geological transitions, their scaling and seismic response. The best correlating atoms are selected from the dictionary via a greedy search algorithm called Matching Pursuit (Mallat, 1997). The dictionary itself, consists of a multitude of *translation-invariant* discrete wavelet transforms (Coifman and Donoho, 1995) computed with respect to order and direction varying fractional spline wavelets. Compared to earlier work (Herrmann, 2001b; Herrmann et al., 2001; Herrmann, 2001a), this approach restores the translation-invariance and allows, via composition, for a singularity/edge preserving reconstruction. Moreover, the atom's parameterization provides information on the location (stratigraphy) and transition abruptness (lithology).

First, we introduce the details of the parametric representation. Then we summarize our method of seismic imaging, followed by the singularity characterization based on the greedy search. We conclude with a multi-component ocean bottom data example (Valhall).

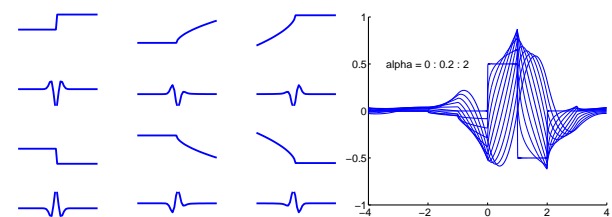


Fig. 1: Example of cusp-like singularities and their seismic response (left) and part of the dictionary (right).

## Parametric representation of geologic transitions

We consider media that consist of accumulations of varying order transitions of the type (Herrmann, 1997, 2001b; Herrmann et al., 2001):

$$\chi_{\pm}^{\alpha}(z) = \begin{cases} 0 & z \leq 0 \\ \frac{z^{\alpha}}{\Gamma(\alpha+1)} & z > 0 \end{cases} \quad (1)$$

with  $\Gamma$  the Gamma function. These depth- $z$  and index- $\alpha$  onset functions define causal  $\chi_{+}^{\alpha}(z)$ , anti-causal  $\chi_{-}^{\alpha}(z)$  and symmetric  $\chi_{*}^{\alpha}(z) = \chi_{+}^{\alpha}(z) + \chi_{-}^{\alpha}(z)$  singularities and are characterized by the parameter  $\alpha$  which determines local scale-invariance of the type,  $\sigma^{-\alpha} \chi_{\pm}^{\alpha}(\sigma t) = \chi_{\pm}^{\alpha}(t)$ ,  $\sigma > 0$ . For  $\alpha = 0$ , the onset becomes a jump discontinuity (piece-wise constant record) and for  $\alpha = 1$  a ramp function (piece-wise linear record). See Fig. 1 for examples. Mathematically, the exponent  $\alpha$  corresponds to the Hölder exponent describing the local differentiability of a function at the transition (Mallat, 1997; Herrmann et al., 2001). The smaller the exponent the sharper, the more abrupt the transition.

In the ray-Born approximation for scattering from non-intersecting smooth interfaces, seismic traces can be represented by a convolutional model (de Hoop and Bleistein, 1997; Herrmann, 2001b). Even though seismic data are bandwidth limited, signatures of the singularities in the medium can be shown to carry through in this model.

## Mapping of geologic singularities by seismic imaging

Recently, a theory of seismic imaging has been developed that transforms data,

$$\mathbf{d}(s, r, t) = \mathbf{K}\mathbf{m} + \mathbf{n} \quad (2)$$

as a function of source ( $s$ ), receiver ( $r$ ) positions and time ( $t$ ) to the scattering position ( $z$ ), angle and azimuth domain ( $\mathbf{e} = (\Psi, \Phi)$ )

$$\mathbf{u}_{\mathbf{x}}(z, \mathbf{e}) = \mathbf{K}^{*}(\mathbf{e})\mathbf{d}(\mathbf{x}, z) \quad (3)$$

with  $\mathbf{u}_{\mathbf{x}}$  a vector with pre-stack migrated data (this vector includes the different wave modes). From now on we suppress references to the horizontal directions ( $\mathbf{x}$ ) in our notation. The noise ( $\mathbf{n}$ ) polluted data in Eq. 2 is assumed to be given by the action of the linearized forward scattering operator ( $\mathbf{K}(\mathbf{e})$ ), acting on the medium elastic perturbations and hence on the geologic record ( $\mathbf{m}$ ). Pre-stack migration as defined in Eq. 3, corresponds to a partial solution of the least-squares inverse problem

$$\langle \mathbf{m} \rangle = (\mathbf{K}^{*} \mathbf{K})^{-1} \mathbf{K}^{*} \mathbf{d} \quad (4)$$

with  $\langle \mathbf{m} \rangle$  a vector with the estimated spatial distribution of the medium perturbation. Formulating the inverse scattering problem in the angles domain naturally reveals the singularity structure even for complicated subsurface models where the waves contain caustics. Eq.'s 3 and 4 map the singularities in the elastic properties. In the domain after imaging (cf. Eq. 3) and prior

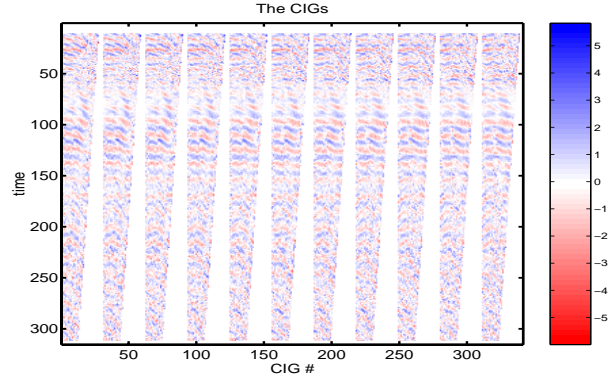


Fig. 2: PP Scattering Angles Common Image Gathers.

to inversion (cf. Eq. 4), reflectors are for each horizontal position images as a function of the scattering angles, see Fig. 2 for examples of the CIG's. These multiple images represent redundancy and provide the appropriate domain for denoising and singularity analysis.

## Singularity detection and characterization

We build a redundant dictionary with atoms that are designed to fit events in a seismic trace in the angles domain. Each event is associated with a wave interaction at a singularity of the type given in Eq. 1

## The Fractional Spline Dictionary

Conventional degree- $m$  splines are piecewise  $m^{th}$ -order polynomials smoothly (for  $m > 0$ ) joined together at the knots. At these knots the  $m^{th}$ -order derivative contains a jump discontinuity. For uniform unit spacing of the knots, splines can uniquely be characterized by a summation of B-splines, which are given by  $m^{th}$ -order auto-convolutions of the boxcar function, i.e.

$$\beta^m(z) = \underbrace{(\beta^0 * \beta^0 * \dots * \beta^0)}_{(m+1) \text{ times}}(z) \quad (5)$$

with  $\beta^0(z)$  being the indicator function on  $z \in (-\frac{1}{2}, +\frac{1}{2})$ . In the Fourier domain this definition corresponds to raising the sinc-function to the  $(m+1)^{th}$ -power. Following Unser and Blu (2000); Blu and Unser (2000), we can generalize integer order splines to fractional  $\alpha$ -order by raising the sinc-function to fractional powers. In the space domain this generalization can be written as the  $\alpha+1$ -order fractional difference of the onset function defined in Eq. 1,

$$\beta_{\pm}^{\alpha}(z) = (\Delta_{\pm}^{\alpha+1} \chi_{\pm}^{\alpha})(z), \quad \beta_{*}^{\alpha}(z) = (\beta_{+}^{\frac{\alpha-1}{2}} * \beta_{-}^{\frac{\alpha-1}{2}})(z) \quad (6)$$

where  $(\Delta_{\pm}^{\alpha} f)(z) = \sum_{k \geq 0} (-1)^k \binom{\alpha}{k} f(z \mp k)$ .

As with ordinary spline wavelets (Mallat, 1997), fractional spline wavelet bases can be constructed via an orthogonalization process (Unser and Blu, 2000), yielding an expression for

the refinement filter. Given this filter we can define the fractional spline wavelets as

$$\psi_{\pm,*}^{\alpha}(\frac{z}{2}) = \sum_{k \in \mathbb{Z}} g_{\pm,*}^{\alpha}[k] \beta_{\pm,*}^{\alpha}(z - k). \quad (7)$$

Compared to ordinary  $m^{th}$ -order spline wavelets,  $\alpha$ -order spline wavelets have a prescribed fractional degree of regularity ( $\alpha$ ) and act as smoothed fractional  $(\alpha + 1)^{th}$ -derivative operators, for the low frequencies ( $\zeta$ ):  $\hat{\psi}_{\pm}^{\alpha}(\zeta) \sim (\pm j\zeta)^{\alpha+1}$  and  $\hat{\psi}_{\pm}^{\alpha}(\zeta) \sim \zeta^{\alpha+1}$  as  $\zeta \rightarrow 0$ . See Kane *et al.* in these proceedings for the application of fractional spline wavelets in the non-linear solution of linear inverse problems using thresholding.

To maintain shift-invariance, we use a wavelet transform with the fractional spline wavelets given by Eq. 7 and without down-sampling. For each  $\alpha$  and direction ( $\{\pm, *\}$ ), we wavelet transform our data, i.e.  $f \mapsto \langle f, \psi_{\pm,*}^{\alpha} \rangle$  with  $\langle f, \psi_{\pm,*}^{\alpha} \rangle$  the empirical wavelet coefficients of  $f$  with respect to the different wavelets.

Compared to the ordinary discrete wavelet transform, the multiple non-downsampled wavelet transforms offer flexibility to find the optimal basis function representation. Optimality, in this case refers to both the regularity-adaptiveness and approximation error as a function of the number of atoms. To reduce the computational cost of finding the best decomposition, we store for each different order and direction the wavelet coefficients into binary trees similar to wavelet packet trees (Coifman and Donoho, 1995), yielding a dictionary  $\mathcal{D} = \{g_{\gamma}\}_{\gamma \in \Gamma}$  with  $g_{\gamma}$  the different  $\alpha$ -order (anti)-causal/symmetric fractional spline wavelets as defined in Eq. 7 (here  $g_{\gamma}$  represent the actual wavelets and not the refinement filters).

### Atomic Decomposition by Matching Pursuit

Following (Mallat, 1997) we use a greedy search algorithm for the decomposition of  $f$  from the redundant dictionary,  $\mathcal{D}$ . This data-adaptive algorithm is based on minimizations of the  $L^2$ -norm difference between reductions of  $f$  and the atoms. Reductions are projections of  $f$

$$f = \langle f, g_{\gamma_0} \rangle g_{\gamma_0} + Rf, \quad (8)$$

where  $Rf$  is the residue and  $g_{\gamma_0}$  the particular  $\gamma_0$ -indexed atom that maximizes the correlation, i.e.  $|\langle Rf, g_{\gamma_0} \rangle| \geq \sup_{\gamma \in \Gamma} |\langle Rf, g_{\gamma} \rangle|$  (Mallat, 1997). The index  $\gamma \in \Gamma$  refers to the location in the tree (dyadic scale ( $2^j$ ) and sample number ( $i$ )), the direction ( $\{\pm, *\}$ ) and the order ( $\alpha$ ). By repeating the above reductions, we obtain the atomic decomposition. Compared to the ordinary wavelet transform, the atomic decomposition specifically depends on the data  $f$ , hence the term data-adaptive.

### Denosing and Reconstruction

In our imaging procedure, the singularities are confined to the spatial direction. Since there are no singularities in the angular directions  $\mathbf{e}$  we may consider the images to be smooth in those directions. In that situation the non-adaptive wavelet transform can be used and good denosing results are obtained when we non-linearly threshold the wavelet coefficients computed for

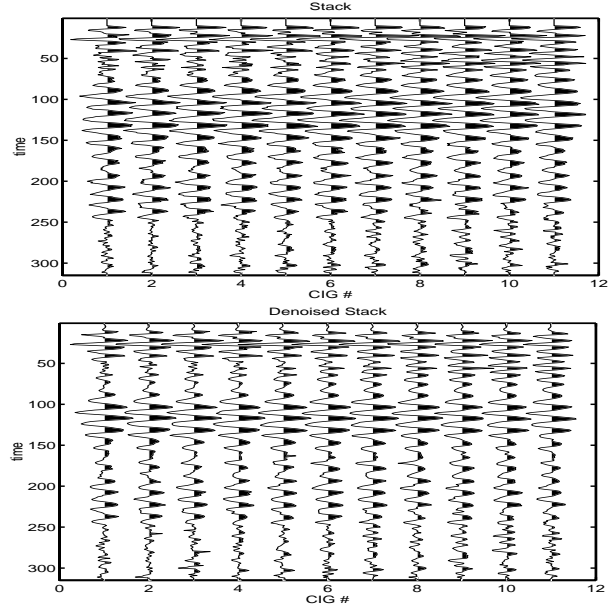


Fig. 3: Comparison ordinary stack and stack after non-linear denosing.

an as smooth as possible wavelet. The non-linear denosed estimates (denoted by the symbol  $\hat{\cdot}$ ) are given by

$$\hat{\mathbf{u}}(\mathbf{e}) = \sum_{\lambda} \theta_j \{ \langle \mathbf{u}, \psi_{\lambda} \rangle \} \psi_{\lambda}(\mathbf{e}) \quad (9)$$

with  $\mathbf{e}$  the angles,  $\theta_j \{ \cdot \}$  the scale-indexed thresholding operator and  $\psi_{\lambda}$  an orthogonal  $\lambda$ -indexed (location ( $i$ ) and scale ( $j$ )) wavelet. After thresholding, the trace by trace continuity is enhanced, a property that is consistent with the data's redundancy. This non-linear thresholding removes the noise and therefore improves the signal to noise ratio in the angles image as well as in the angular stack and inversion.

Since the singularities are located in the spatial direction we apply our matching pursuit algorithm on each angular trace. This algorithm gives us, for each angle, a decomposition into a noise level dependent number ( $M$ ) of atoms. Reconstruction of  $\mathbf{u}(z)$  by these first  $M$  atoms,

$$\hat{\mathbf{u}}(z) = \sum_{m=1}^M \langle \mathbf{u}, g_{\gamma_m} \rangle g_{\gamma_m}(z). \quad (10)$$

gives us the denosed estimate as long as we choose  $M$  such that  $\frac{|\langle R^M \mathbf{u}, g_{\gamma_M} \rangle|}{\|R^M \mathbf{u}\|} > \text{noise level}$ . By construction, the selected atoms can be interpreted as data-adaptive ‘‘principle geologic components’’. For seismic reflectivity, the wavelet coefficients of the noise and reflectivity are very close and hence **not** seperable, rendering non-data adaptive wavelet thresholding techniques ineffective. However, redundancy in our dictionary allows us to find the coherent structures.

In Fig 3, we present the results of denosing followed by stacking. We can see that the denosing significantly improves the resolution especially at the reservoir (just below sample # 100).

## Singularity characterization

The atom's parameterization provides estimates for the location, order, direction and scale of the reflectors. These parameters are given by the parameterization of the selected atoms. Fig. 4 summarizes the estimates which correspond to the first 100 selected atoms. Notice the reasonable lateral consistency.

## Implications for modeling and interpretation

We conclude from our example that discontinuities other than zero-order steps and first-order ramp functions occur in the earth. This observation has important consequences for the interpretation of geological boundaries, which can not longer be considered as strictly local as is the case for jump discontinuities. By construction, our decomposition is equivalent to a fractional spline representation for the geological record, where the location and singularity orders of the knots correspond to the location (stratigraphy) and transition abruptness (lithology). Since the atoms represent the coherent structures in the data we can suppress GRT artifacts and hence improve image quality, while preserving the singularities. Finally, the decomposition opens the way for an data-adaptive atomized formulation of seismic imaging and inversion.

## Acknowledgement

This work was supported by ERL Founding Members Consortium. The authors wish to thank Dr. Sverre Brandsberg-Dahl of BPAmaco for providing the migrated data.

## References

- Thierry Blu and Michael Unser. The fractional spline wavelet transform: Definition and implementation. In *Proceedings*, volume I, pages 512–515. IEEE, 2000.
- S. Brandsberg-Dahl and M. de Hoop. Focusing in dip and ava compensation on scattering-angle/azimuth common image gathers. *Geophysics*, 1998.
- R. R. Coifman and D. L. Donoho. Translation-invariant de-noising. Technical report, Department of Statistics, 1995. URL [citeseer.nj.nec.com/80329.html](http://citeseer.nj.nec.com/80329.html).
- Maarten de Hoop and Norman Bleistein. Generalized radon transform inversions for reflectivity in anisotropic elastic media. *Inverse Problems*, 13(3):669–690, 1997.
- David L. Donoho and Iain M. Johnstone. Minimax estimation via wavelet shrinkage. *Annals of Statistics*, 26(3):879–921, 1998. URL [citeseer.nj.nec.com/donoho92minimax.html](http://citeseer.nj.nec.com/donoho92minimax.html).
- Felix J. Herrmann. Fractional spline matching pursuit: a quantitative tool for seismic stratigraphy. In *Expanded Abstracts*, Tulsa, 2001a. Soc. Expl. Geophys. URL <http://www-erl.mit.edu/~felix/Preprint/SEG01.ps.gz>.
- Felix J. Herrmann. Singularity Characterization by Monoscale Analysis: Application to Seismic Imaging. *Appl. Comput. Harmon. Anal.*, 2001b. to appear March/June 2001.

Felix J. Herrmann, William Lyons, and Colin Stark. Seismic facies characterization by monoscale analysis. *Geoph. Res. Lett.*, 28(19):3781–3784, Oct. 2001. URL <http://www-erl.mit.edu/~felix/Preprint/WellSeis.ps.gz>.

F.J. Herrmann. *A scaling medium representation, a discussion on wells, logs, fractals and waves*. PhD thesis, Delft University of Technology, Delft, the Netherlands, 1997. URL <http://wwwak.tn.tudelft.nl/felix>.

S. G. Mallat. *A wavelet tour of signal processing*. Academic Press, 1997.

J. Muller, I. Bokn, and J. L. McCauley. Multifractal analysis of petrophysical data. *Ann. Geophysicae*, 10:735–761, 1992.

Michael Unser and Thierry Blu. Fractional splines and wavelets. *SIAM Review*, 42(1):43–67, 2000.

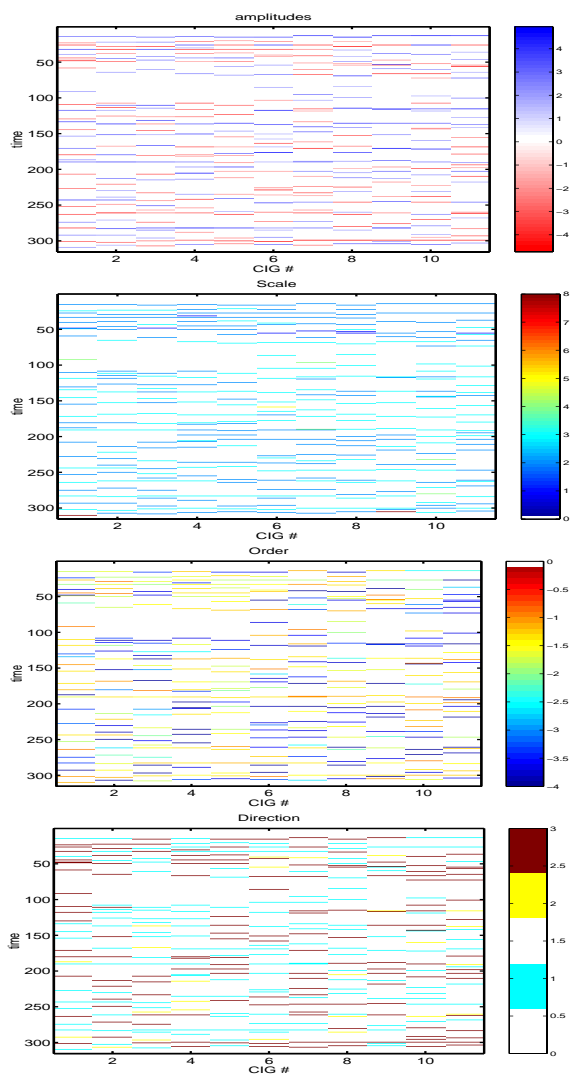


Fig. 4: Estimated amplitudes, scale, order and direction (1 anti-causal, 2 symmetric and 3 causal) respectively.